Geometric factors influencing the optimal position of geogrid reinforcement

D.H. Marx
University of Pretoria, South Africa (marxdavidh@gmail.com)

S.W. Jacobsz
University of Pretoria, South Africa (sw.jacobsz@up.ac.za)

ABSTRACT: The behaviour of geogrid-reinforced clay liners, subject to differential settlement, was investigated using finite element (FE) analyses. The optimal geogrid reinforcement strategy for a liner was determined by generating a Pareto front of maximum liner tensile strain versus total cost of reinforcement. To conduct the number of FE analyses required as input for the optimisation algorithm would have been too expensive. Thus, a surrogate surface was generated with a limited number of FE analyses. This surface was used to interpolate the problem's response. The optimal reinforcement strategy (ORS) was found to be insensitive to landfill height (overburden pressure) and the clay liner thickness. The width, depth and shape of the imposed settlement trough did however influence the ORS. These preliminary results recommends reinforcement of the liner at both the bottom and the top quarter.

Keywords: piggyback landfill, optimisation, Pareto front, geogrid, finite element modelling

1 INTRODUCTION

Continued population growth places strain on current waste disposal facilities in South Africa. Limited air space suitable for landfilling, however, drives the need for alternative solutions to expand waste disposal capacity. One such solution is the vertical extension of current landfill sites (i.e. piggyback landfills). This method entails building a new, fully lined, landfill on top of the existing waste. The old underlying general municipal waste, however, is prone to local and differential settlement (see for example El-Fadel & Khoury (2000)). Settlement of this waste will result in the clay liner bending, and eventually cracking. Consequently, some form of tensile reinforcement is required in the clay.

Geogrids can be used to reinforce the clay by disrupting the tensile strain fields that develops (Jones, 1985) and by providing support to the clay liner. Marx & Jacobsz (2016) conducted a numerical study to investigate the optimal geogrid reinforcement positions in a simple clay liner, subject to differential settlement. The current paper is an extension of that work, investigating the influence of various geometric factors on the optimal reinforcement strategy (ORS). The ORS is defined as the positions in the liner where reinforcement should be placed to minimise liner tensile strain, for a given reinforcement cost. Furthermore the ORS also includes the proportion of total reinforcement cost to be expended at each of these positions.

It is therefore intended to optimise the position(s) within the liner at which to place the geogrid(s). This is done by minimising the maximum tensile strain generated in the liner by an imposed differential settlement profile; given a total cost of reinforcement. To summarise: the ORS entails the optimal position of geogrids, and stiffness at that position, given a maximum reinforcement cost.

To better understand the problem the influence of a couple of key factors on the behaviour of the liner was investigated. These are: the overburden pressure applied; clay liner thickness; magnitude of central settlement, and the width and shape of the settlement trough developing in the underlying waste body. Each of these factors is a key consideration for piggyback landfill design:

- The height of the landfill changes during the lifetime of the landfill (due to construction but also consolidation of the waste). This, combined with the inherent variability in the unit weight of the waste (Kavazanjian 2001; Zeccos 2005), results in highly variable overburden pressure. For the remainder of the article the variation in height of the landfill will be represented by a change in overburden pressure.
- The thickness of the landfill liner is usually prescribed by a national standard. However, when conducting model studies in a geotechnical centrifuge at high gravitational acceleration, the dimensions of the required model may result in it being quite fragile (12mm model at 50G representing a 600mm prototype). Should the ORS prove to be insensitive to the liner thickness, more practical models can be used.
- The width and shape of a settlement trough occurring in a landfill depends on the occurrence of local voids and differential settlement. Both factors are difficult to measure in practice and not well understood.

2 FINITE ELEMENT ANALYSES

To investigate the influence of the various factors identified on the ORS of the clay liner, a number of different finite element (FE) models were analysed. These plane strain problems were analysed in ABAQUS 6.13-3. The modelling approach was validated against the centrifuge models of Rajesh & Viswanadham (2011, 2012).

2.1 *General model*

The key parts of the model is presented in Figure 1. These are:

1. *A clay liner* of thickness *4t* and half-width b+c = 25 m, where c is the width of half the settlement trough. Between 4272 to 6768 continuum, plane strain, eight-node (CPE8) elements were used to model this liner. An isotropic linear elastic undrained Mohr-Coulomb plasticity model was used.

2. *Four possible positions of geogrid reinforcement* were considered. The South African standard for landfill design (DWAF, 1998) requires that the clay liner should be compacted in four distinct layers. The interface between these layers were identified as the possible reinforcement positions. 333 to 423 two-node truss (T2D2) elements were modelled as linear elastic for each of the geogrids.

   The interaction between the geogrid and the clay was modelled by merging coinciding geogrid and clay element nodes. Accordingly, the displacement at any of the merged nodes depends on both the clay element and the stiffer geogrid element. This models the reinforcing effect. The assumption holds while there is compatibility between the geogrid and the clay. Since the problem was modelled only up to the onset of fracture at the base or surface of the clay, this assumption is deemed reasonable (considering

that the strain in a beam in bending increases from the neutral axis to the surface). Furthermore, Rajesh & Viswanadham (2015) found that the response of their model was largely insensitive to the interface coefficient modelled between the geogrid and the clay. Koutsourais et al. (1991) found that for geogrids with large apertures the interactional properties is similar to that of the soil.

3. *The contact surface with the underlying waste body*. The surface of the waste body was set to displace according to a predefined settlement profile. This simulates the presence of a void below the liner. The waste surface and the clay liner was modelled as separate parts and the contact was assumed to be frictionless as this is the most conservative modelling option. A frictional surface would confine the clay, inhibiting the clay elements from moving apart. Thus, lowering the tensile strain.

In terms of boundary conditions, movement in the horizontal direction was prevented at the right hand side of the model, modelling symmetry. The same boundary condition was applied at the left hand side.

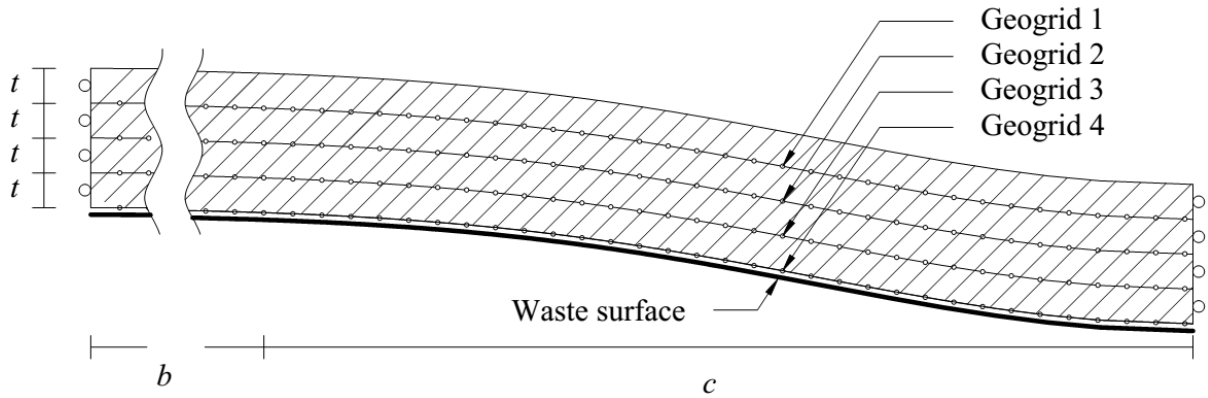

Figure 1 - General geometry of FE models analysed

2.2 *Validation model*

The material models and reinforcement modelling approach discussed in the previous section were validated against the centrifuge models of Rajesh & Viswanadham (2011, 2012). A comparison with the numerical models of Rajesh & Viswanadham (2015) is also presented. These models represented a 1.2m clay liner, 28m long, with a settlement trough of 16m width. The clay had a density of 1447 kg/m^3, a secant Young's Modulus of 2620 kPa, Poisson ratio of 0.3 and an undrained shear strength of 19 kPa. The clay liner was reinforced at the top quarter with a geogrid of stiffness 10 000 kN/m and Poisson ratio of 0.3. A 25 kPa overburden pressure was applied.

These same material properties and overburden pressure were implemented for validation of the modelling approach of the current study. Assuming a density of 1500 kg/m^3 for the clay (equivalent to consolidation pressure of 630kPa (Jessberger 1991)) the tensile strength of the compacted clay ranges between -37.65kPa (Thusyanthan et al. 2007) and -15 kPa (Tang et al. 2014). Modelling a tensile cut-off of this magnitude had only a minor effect on the strain behaviour while increasing the computational effort significantly. Accordingly, no tensile cut-off was modelled. This assumption is only valid for central settlements of limited extent (in this case < 1m).

Rajesh & Viswanadham (2011, 2012) used a trapdoor to induce a 16 m settlement trough to the liner. It is assumed for this study that the deformed profile of the clay followed the Gaussian curve of Martos (1958) (see Equation 1). Accordingly, the waste surface underlying the clay liner was displaced in the shape of this profile for validation. The parameter *i* (the distance

from the centre to the point of inflection) is equal to a fifth of the trough width (New & O'Reilly, 1991) and was therefore set to 3.2 m (for a trough width of 16 m).

$$s = s_{max} \cdot e^{-\frac{x^2}{2i^2}} \tag{1}$$

The liner thickness was set to 1.2 m (i.e. t = 0.3 m). As with Rajesh & Viswanadham (2015) the geogrid was placed one quarter of the thickness (0.3 m) from the top of the liner. This was modelled with geogrids of stiffness 0kN/m at positions 2-4 (see Figure 1) and a stiffness of 10 000 kN/m at position 1.

In landfills the length of the geogrid used will ensure sufficient lateral anchoring. However, in the centrifuge models of Rajesh & Viswanadham (2011, 2012) the model geogrids were not anchored at their edges. Slight separation of the model from the walls of the strong box could occur in the centrifuge. Accordingly, for the validation of the modelling approach the horizontal restraint at the left edge of the general model (see Figure 1) was removed.

The maximum tensile and compressive strains predicted by the numerical validation model of this study, at the surfaces of the clay liner, for different central settlements are shown in Figure 2. Both the results of the reinforced and the unreinforced models are compared to the centrifuge models of Rajesh & Viswanadham (2011, 2012) and the numerical analysis of Rajesh & Viswanadham (2015). It is assumed that the strain results of the centrifuge models is presented as nominal (engineering) strain. The numerical model of the current study captures the trend of the physical model adequately.

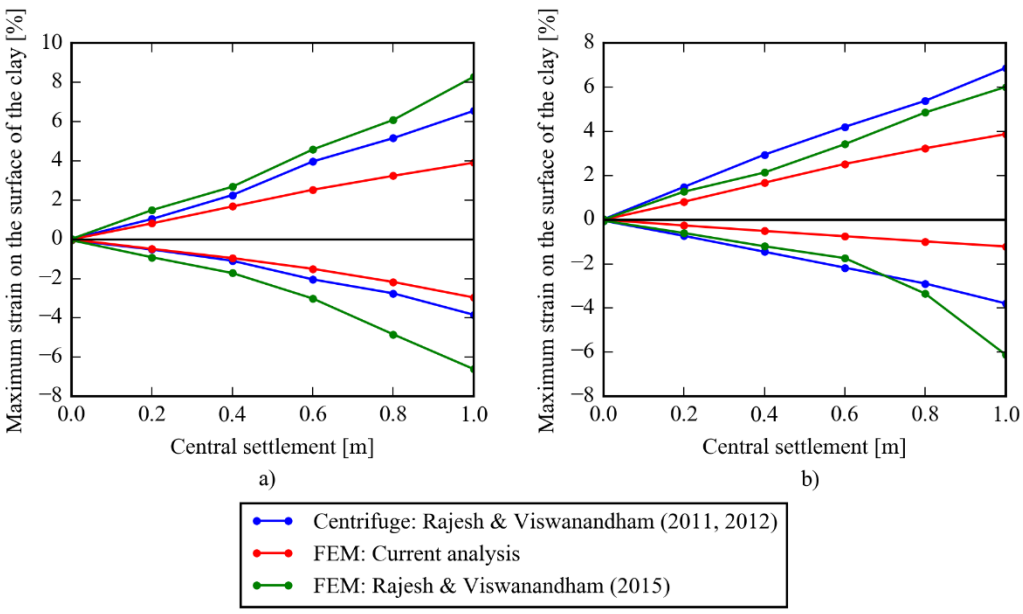

Figure 2 - Validation of the FE model. Greatest nominal strain at the surface of a) the unreinforced clay liner and b) the geosynthetic reinforced clay liner. Compressive strain is positive and tensile strain is negative.

2.3 *Models analysed*

A "standard" FE model was set up to be used as baseline for comparison in the subsequent sensitivity analyses. This model had a total width of 50 m (25 m modelled), a Gaussian settlement trough (i = 3), total trough width of 15 m (2b – Figure 1), maximum central settlement of 1m, liner thickness (4t) of 1 m and an overburden pressure of 25 kPa (representing the landfill cover). The material models and properties of the standard model, and all subsequent models, were the same as those for the validation model. A summary of the models (or problems)

analysed to investigate the influence of the factors identified earlier, and their deviation from the standard model, is presented in Table 1.

Table 1. Models optimised and their respective deviation from the standard model

Model name	Variation from standard model
0.5m thick liner	Liner thickness of 0.5m
1.5m thick liner	Liner thickness of 1.5m
0kPa overburden	No overburden pressure
50kPa overburden	50kPa Overburden pressure

Model name	Variation from standard model
5m trough	5m wide settlement trough (c = 2.5 m)*
25m trough	25m wide settlement trough (c = 12.5 m)*
Generalised bell	Settlement trough shaped as a generalised bell curve

*c indicated in Figure 1

3 PARETO FRONT GENERATION

To determine the optimum reinforcement strategy, objectives (criteria) to measure the performance of the designs against needs to be established. Two such objectives were identified: 1) the total cost of reinforcement and 2) the maximum tensile strain in the liner (assumed to be indicative of cracking and thus the permeability/performance of the liner). For the purposes of this work the cost of reinforcement was assumed to be equivalent to the sum of geogrid stiffnesses

A lower cost and a lower maximum tensile strain would both be indicative of a good design. However, these two objectives are in conflict – reducing the total reinforcement (i.e. cost) increases the tensile strain and vice versa. Accordingly, one can isolate a number of designs, where for a given cost no other design exists that results in a lower maximum tensile strain. This front of objective values that emerges is known as a Pareto Front. Given two objective functions (criteria), for any point on the Pareto front reducing the one objective function will increase the other

Numerous strategies exists to isolate these Pareto fronts. For the current project the DEAP (Distributed Evolutionary Algorithms in Python) software package (Fortin et al. 2012) was used to implement the NSGA-II algorithm (Deb et al. 2000). The NSGA-II algorithm was chosen for its ease of use (only one tuning parameter) as well as its efficiency (Konak et al. 2006).

The Pareto optimal front for the standard model is presented in Figure 3. The data presented is a 15 point forward and backward moving average. As the cost of reinforcement is assumed to be equivalent to the stiffness of the geogrid, the horizontal axis displays tensile stiffness in lieu of cost. The maximum cost (stiffness) of reinforcement at any of the four positions considered (indicated in Figure 1) was limited to 2.5 MN/m.

The optimal reinforcement for a given total reinforcement cost (stiffness) can be determined from Figure 3 as follows. Consider a total reinforcement cost of 2 MN/m. The minimum possible tensile strain in the liner, for that cost, is 2.7%. To attain that strain one has to allocate 31% of the cost to the geogrid in position 1 and 69% of the cost the geogrid in position 4. That is, a geogrid of stiffness 0.615 MN/m in position 1 and a geogrid of stiffness 1.385 MN/m in position 4. This allocation in cost (stiffness) is the optimal reinforcement strategy (ORS) defined earlier. For the remainder of the paper only the percentage of the total cost allocated to each position will be presented, and not the actual stiffness.

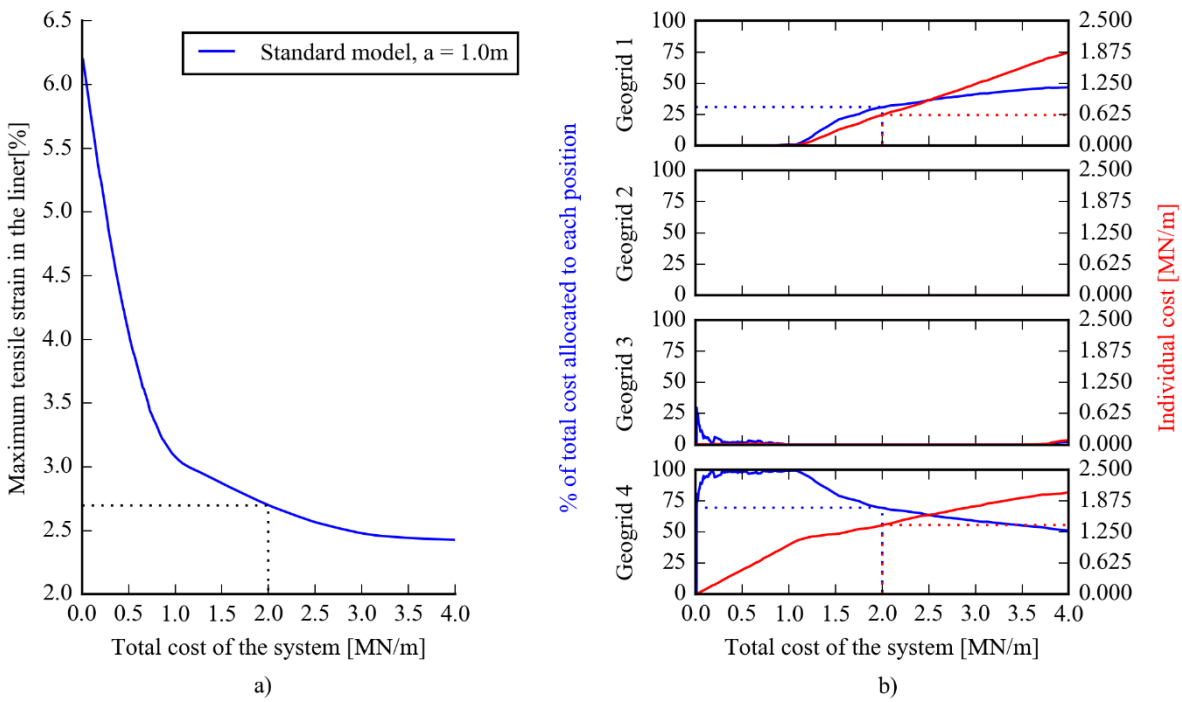

Figure 3 - Pareto optimal front (a) and corresponding ORS (b) for the standard model

4 SURROGATE SURFACE GENERATION

To determine the reinforcement strategy for the sensitivity analyses, numerous combinations of geogrid stiffnesses (designs) had to be analysed. Conducting a FE analysis for every possible design is impractical. Even conducting analyses only for the designs that the search algorithm evaluates is impractical. Consequently, the influence of only a number of designs on the maximum tensile strain was evaluated with a FE analysis. A surface was fitted to these points to allow for interpolation of the maximum strain at the remaining designs. The surface used was a radial basis function surface (RBF) with Gaussian base functions were (Forrester & Keane 2009).

Each RBF was generated from 900 different FE analyses. The stiffnesses for each design was generated randomly. Using a uniform distribution to sample the designs could have resulted in some regions of the sampling space being under-represented. Accordingly, Latin Hypercube Sampling (LHS) was implemented (Ross, 2013). With LHS the sampling space is divided into *n* discrete segments. Subsequently, a uniform random sample is generated from each segment. Further manipulations are applied to ensure that, for a given vector, all components originate from different segments. Accordingly, this method ensures that the entire sampling space is well represented.

The RBF surface fitted to the results of the FE analyses has a single tuning parameter, ε. This parameter was adjusted to improve the fit of the RBF to the modelled data and thus lower the prediction error. Ninety percent of the FE results were used to fit the RBF and the remaining 10% to calculate the prediction error, as suggested by Hastie et al. (2001). This process was repeated 10 times, each time using a different subset to calculate the prediction error. The ε-value was adjusted until the summed error was minimised. This ε-value was subsequently used to generate the RBF.

In a similar manner the generalisation error made by the RBF (that is the error made predicting data other than the training set) can be calculated. For each problem 85% of the data was used to train the RBF while the prediction error was calculated for the remaining 15% of the data. For all problems considered the mean RMSE of the prediction error was 0.037% strain, while the standard deviation was 0.042% strain. Since all 900 designs (and not only 85%) were used to construct the RBFs used in the subsequent sections, it is assumed that the actual generalisation errors are even lower. It was found that the higher the prediction error of the RBF the more difficult it was to generated a full set of Pareto optimum designs (see next section)

5 RESULTS AND DISCUSSION

The results of the sensitivity analyses are divided into two categories: those factors that did not have any distinct influence on the liner ORS (overburden pressure and clay liner thickness); and those that had (degree of central settlement, trough width and shape).

Compacted clay liners are generally heavily over-consolidated. Therefore the liners will crack at fairly low strains (LaGatta et al., 1997). Consequently, it is assumed that the mass of clay will behave elastically prior to cracking. Accordingly, the strain distribution in the liner can be approximated using elastic beam theory to facilitate understanding of the problem:

$$\varepsilon(x,y) = \kappa y = \frac{d^2 s}{dx^2} \cdot y \qquad (2)$$

where s is the deflection at position x and y the distance from the neutral axis of the beam and κ the curvature of the beam.

5.1 *Variables with no influence on the optimum reinforcement strategy: overburden pressure and liner thickness*

Clay is ductile and has little capacity to arch over voids. Consequently, as the waste settles the clay will distort in the shape of the deformed waste surface, without spanning the void. Higher overburden pressure will not increase the distortion of the liner as it is already at the maximum possible under self-weight. Thus, the general shape of the strain distribution will remain unchanged. Considering that the clay is heavily overconsolidated the compression due to increased overburden pressure is slight. Thus, it is not expected that the overburden will have an influence on the optimum reinforcement strategy of the liner. The numerical results supports this statements. In Figure 4 it can be seen that the optimum reinforcement strategy is the same for the three different overburden pressures considered.

The maximum strain in the liner, however, is influenced by the overburden pressure. Due to the confining effect of the pressure crack propagation is inhibited (Jessberger, 1991), however the occurrence of cracks is not suppressed. Neither is the strain due to bending reduced. On the contrary the additional stress will strain the liner slightly more, translating the Pareto optimal front upwards (i.e. higher strain) for overburden pressure above 0 kPa (see Figure 4). The variation in overburden was, however, relatively small and did not have a significant effect on the Pareto front.

The strain at the surface of an elastic beam (see Equation 2) depends on the distance to the neutral axis. As with a change in overburden, a change in thickness of the liner is assumed not change the deflected shape, and by implication the distribution of strain in the liner. Accordingly, the thickness of the clay liner does not have an influence on the reinforcement strategy. However, the strain at the outer extremities of the liner is proportional to the distance from the neutral axis (see Equation 2 and Viswanadham & Rajesh (2009)). Jessberger et al. (1989) found that the distortion required for tensile cracking was a function of liner thickness.

Accordingly, with increased liner thickness the maximum strain increases and the Pareto front will translate upward. In Figure 4 the Pareto front, as well as optimal design strategy is shown for clay liners of thickness 0.5 m, 1 m (standard liner) and 1.5 m. These results, supports the aforementioned reasoning.

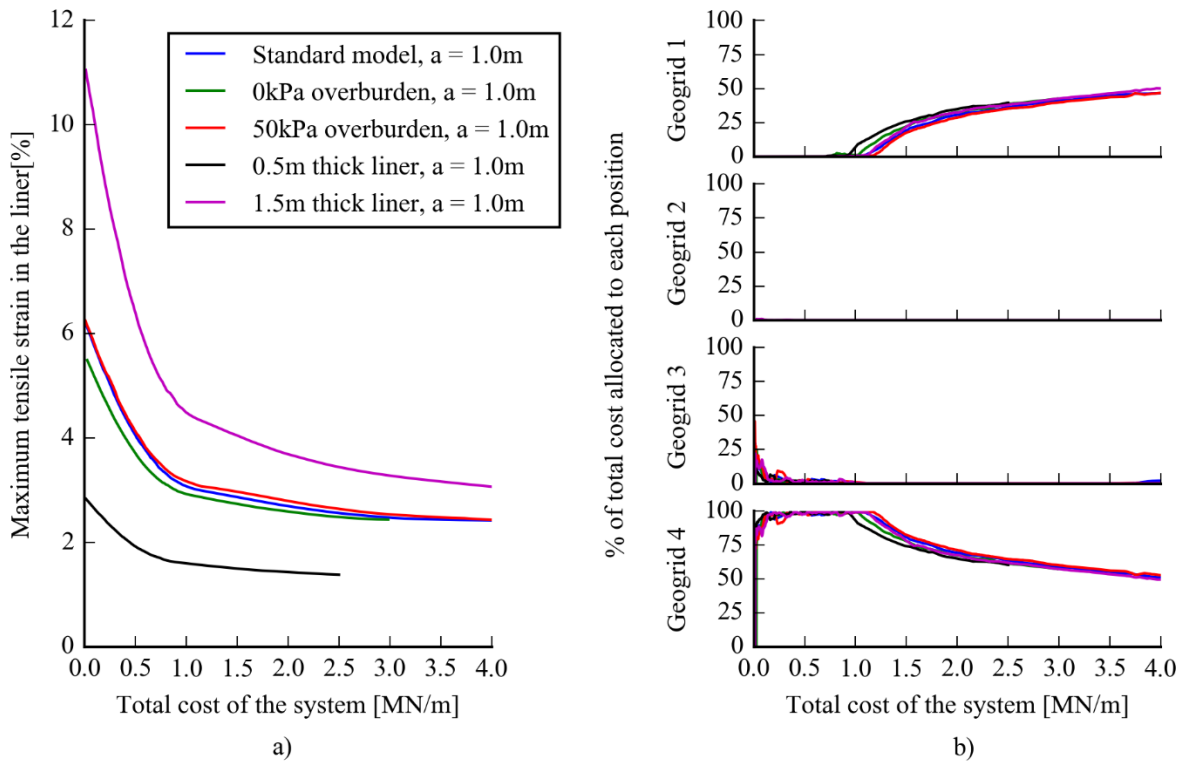

Figure 4 – Pareto front (a) and corresponding ORS (b) of the standard model, models with varying overburden pressure and models with varying liner thickness

5.2 *Variables affecting the optimum reinforcement strategy: problem geometry*

5.2.1 *Central settlement*

The strain distribution with depth in an elastic beam depends on the curvature of the beam at that position. Consequently, for an increase in central settlement of the liner increases the deflected profile changes and the ORS will change accordingly. In Figure 5 the Pareto front and ORS for the standard liner for different degrees of central settlement (*a*) are presented.

As expected, the ORS differs for the varying central settlements. However, the optimal geogrid positions does not change (top quarter and bottom) as evident in Figure 5. Only the distribution of resources (summed stiffness) varies. As the central settlement increases more reinforcement is required at the top quarter of the liner. For the same total cost a liner that settled 1m requires more reinforcement at the top quarter than one undergoing 0.4m of settlement.

A possible interpretation for this behaviour is provided. Consider the two mechanisms of geogrid reinforcement: load sharing and disruption of the tensile fields. At low central settlement a significant reduction in tensile strain is achieved with the inclusion of reinforcement, sharing of the load between the clay and the geogrid. However, as the central settlement, and thus the curvature of the liner increases, a greater reduction in strain is achieved by disruption of tensile strain by the reinforcement. Accordingly, the importance of reinforcing at top quarter depth increases due to the higher strain at the concave part of the trough.

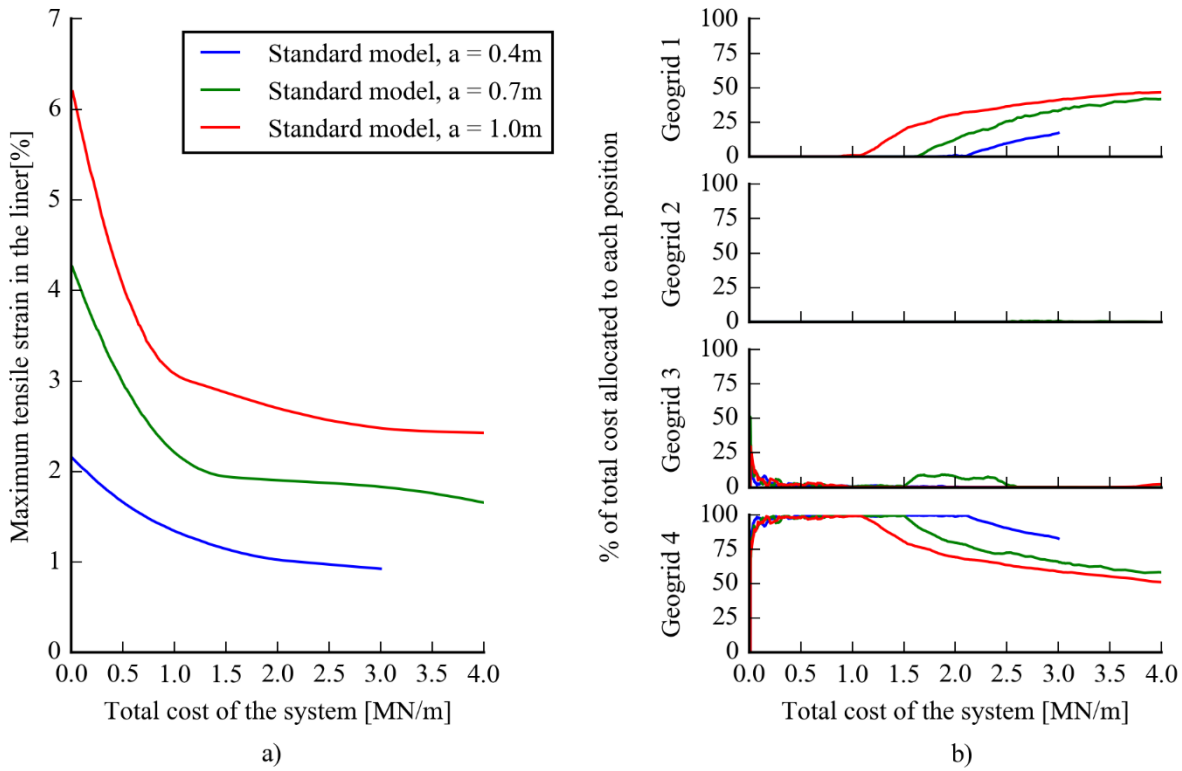

Figure 5 – Pareto front (a) and corresponding ORS (b) for the standard model for varying degrees of central settlement

5.2.2 *Trough width*

Beams (or liners) with the same curvature is assumed to have the same strain distribution, independent of the beam size (see Equation 1). The curvature, or distortion, is a function of the central settlement (a) and the settlement trough width (2*l*). LaGatta et al. (1997) defined this relationship as the distortion level (*a/*). This relationship can be used to define the behaviour of distorted liners and allows for comparison.

The curvature, however, does not depend only on the ratio between the central settlement and trough half-width. Consider the expression for the curvature of the Gaussian curve used earlier as defined in Equation 2.

$$\kappa = \frac{d^2 s}{dx^2} = \frac{2.5 i S_{max}}{\sqrt{2\pi}\, i^3}\left(\frac{x^2}{i^2} - 1\right) e^{-\frac{x^2}{2i^2}} = \frac{2.5\left(\frac{w}{5}\right) S_{max}}{\sqrt{2\pi}\left(\frac{w}{5}\right)^3}\left(\frac{x^2}{\left(\frac{w}{5}\right)^2} - 1\right) e^{-\frac{x^2}{2\left(\frac{w}{5}\right)^2}} \qquad (2)$$

Thus, the curvature is also a function of the magnitude of central settlement and trough width, and not only the ratio thereof. Furthermore, Gabr and Hunter (1994) found that the tensile strain cannot be uniquely defined by the distortion level only. Both the overburden pressure (as discussed earlier) and the trough width should be considered. Accordingly, the distortion level alone might prove inadequate in describing the strain behaviour of clay liners.

In Figure 6 the Pareto front, and corresponding ORS, is presented for troughs of varying widths, and the same *a/l* ratio of 0.093. Other distortion ratios was also investigated and found to behave similar. The Pareto fronts differs distinctly for the various trough widths. This suggests that the strain magnitude generated differs as a function of trough width, even though the distortion level is the same. For all ORSs, however, geogrids are required at the bottom of the liner and at the top quarter depth, specifically with the stronger geogrid at the bottom of the liner.

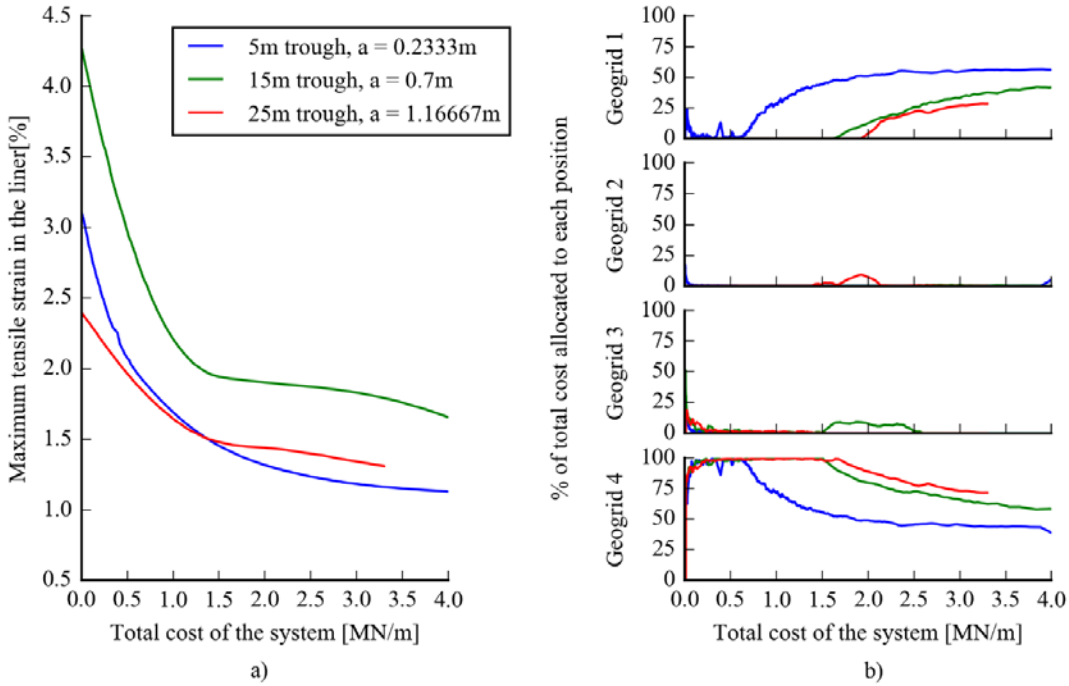

Figure 6 - Pareto front (a) and ORS (b) for troughs of varying widths and shape, with a/l = 0.09333

5.2.3 *Trough shape*

The standard modelled the profile of the settled waste as a Gaussian curve. This shape is, however, only an assumption. The actual settlement trough may have a more random shape. To investigate the influence of trough shape on the ORS, the waste profile underlying the liner was also modelled to deform in the shape of a generalised bell curve (see Equation 3). The parameter *m* can be proven to be equal to the distance to the inflection point of the curve. Accordingly, *m* was set to be equal to 3, to have same inflection point as the standard model. The parameter *n* was set to 2 to model a steeper profile than to the standard Gaussian curve (see Figure 7). The resulting Pareto fronts and ORSs are compared to the standard curve in Figure 8, for a trough width of 15m and various degrees of central settlement. There is some noise in the ORS results, however, clear observations can be made.

$$s = s_{max} \frac{1}{1 + \left|\frac{x}{m}\right|^{2n}} \tag{3}$$

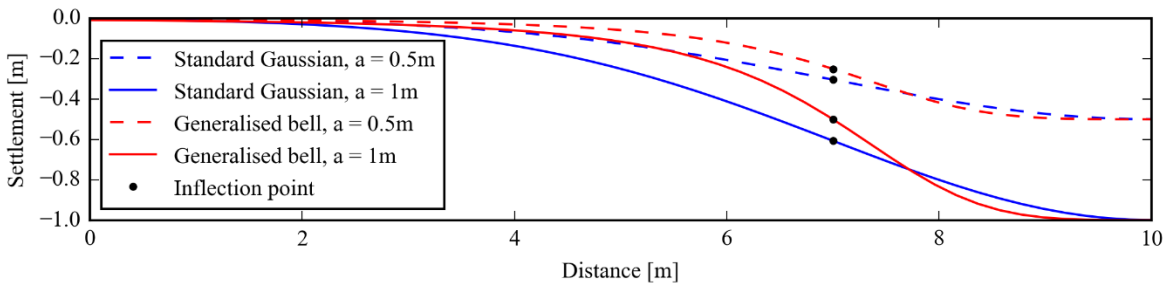

Figure 7 – Shape of the settlement trough for the standard and generalised bell curves, for different central displacements

The ORS differed significantly for the two settlement troughs. Even though both ORSs comprises mainly of reinforcement only at the top quarter (position 1) and bottom (position 4), the relative importance differs. For example reinforcing at the top (position 1) rather than at the bottom is significantly more important for the generalised curve. Additionally, reinforcement

at both positions is required for almost all costs. In contrast for Gaussian settlement reinforcement is required at the top only after the stiffness in the first layer reaches the maximum.

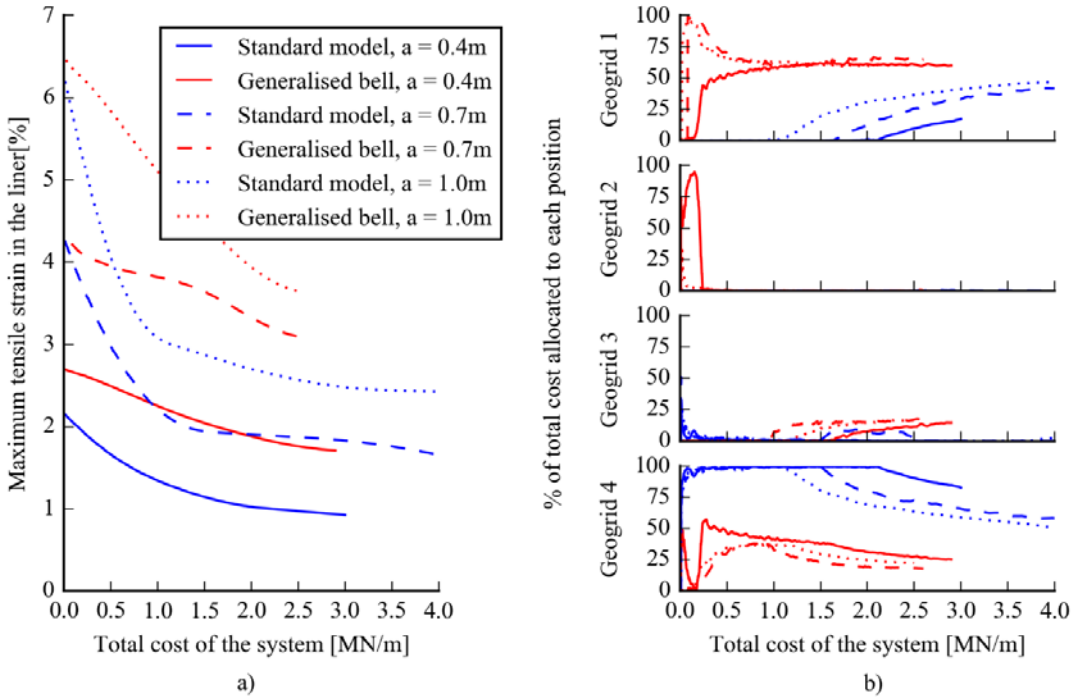

Figure 8 - Pareto optimal front (a) and ORS (b) for both the standard and generalised bell curves, for a number of central settlements.

Richards & Powrie (2011) found that the shape of the subsidence pattern had a significant influence on the hydraulic conductivity of a liner. Interestingly, they found that a liner subject to a more jagged distortion profile resulted in poorer performance than a liner subject to smoother one. The steeper distortion corresponds to shearing of the liner and therefore a significant impairment in functionality. Likewise the current analysis found that the generalised bell profile resulted in Pareto optimal fronts of greater strain, compared to the equivalent Gaussian profiles, requiring greater expense in terms of reinforcement cost.

6 CONCLUSIONS

The optimal reinforcement strategy for a clay liner subject to differential settlement was investigated. It was found that neither the overburden pressure nor the liner thickness influenced the ORS. The reinforcement strategy for the standard problem (15m Gaussian trough, 1m thick liner and 25kPa overburden pressure) primarily comprised of a geogrid at the bottom of the liner, with an additional geogrid at top quarter depth as more resource became available.

Trough width and shape, as well as central settlement, however, did have an influence on the ORS. For these parameters is was found that the addition of reinforcement at the top quarter of the liner is of importance (compared to the standard model). Furthermore, the ORS is highly sensitive to the shape of the settlement profile. For a steeper, generalised bell shaped settlement trough reinforcement at the top quarter depth of the liner was of the greatest importance. For almost any cost the optimal reinforcement strategy entails a two-level approach.

A conservative design, that is insensitive to the factors considered, would consists of two-level geogrid reinforcement. This is, however, only a preliminary recommendation and further work has to be conducted.

7 ACKNOWLEDGEMENTS

The financial assistance of the Deutscher Akademischer Austausch Dienst (DAAD), the National Research Foundation of South Africa (NRF) and the Geosynthetics Interest Group of South Africa (GIGSA) is acknowledged by the first author. Opinions expressed and conclusions presented are those of the author and are not necessarily to be attributed to the NRF or GIGSA.

8 REFERENCES

Deb K, Agrawal S, Pratap A, Meyarivan T. A fast elitist non- dominated sorting genetic algorithm for multi-objective optimization: NSGA-II. In: *Proceedings of sixth international conference on parallel problem solving from nature*, 18–20 September, 2000. Paris, France: Springer; 2000

Kavazanjian, E., 2001. Mechanical properties of municipal solid waste. *In Proceedings Sardinia – 8th International Waste Management and Landfill Symposium, Cagliari, Italy* V3 pp. 415-424.

Konak, A., Coit, D.W., and Smith, A.E. 2006. Multi-objective optimization using genetic algorithms: A tutorial. *Reliability Engineering and System Safety* V9(91): 992-1007.

Forrester, A. & Keane, A. 2009. Recent advances in surrogate-based optimization. *Progress in Aerospace Sciences* 45(1-3): 50–79

Fortin, F.-A., De Rainville, F.-M., Gardner, M.-A., Parizeau, M., and Gagné, C. 2012. DEAP: Evolutionary Algorithms Made Easy. *Journal of Machine Learning Research* V13: 2171-2175

Gabr, M. A., & Hunter, T. J. 1994. Stress-strain analysis of geogrid-supported liners over subsurface cavities. *Geotechnical & Geological Engineering*, 12(2), 65-86.

Hastie T, Tibshirani R, Friedman J. 2001. *The elements of statistical learning*. New York: Springer.

Jessberger, H. & Stone, K. 1991. Subsidence effects on clay barriers. *Geotechnique* 41(2): 185–194

Jones, C. 1985. *Earth Reinforcement and Soil Structures*. Butterworth and Co. Ltd

El-Fadel, M. and Khoury, R. 2000. Modeling settlement in MSW landfills: a critical review. *Critical reviews in environmental science and technology*, 30(3), pp.327-361.

Jessberger, H.L., Giittler, U. and Stone, K.J.L. 1989. Centrifuge modelling of subsidence effects on clay barriers. *In Proc. 2nd Int. Landfill Symp. Sardinia*.

Koutsourais, M.M., Sprague, C.J. and Pucetas, R.C. 1991. Interfacial friction study of cap and liner components for landfill design. *Geotextiles and Geomembranes*, 10(5), pp.531-548.

LaGatta, M. D., Boardman, B. T., Cooley, B. H., & Daniel, D. E. 1997. Geosynthetic clay liners subjected to differential settlement. *Journal of Geotechnical and Geoenvironmental Engineering*, 123(5), 402-410.

Martos, F. Concerning an approximate equation of subsidence trough and its time factors. *International Strata Control Congress*, Leipzig. pp 191-205

New, B. & O'Reilly, M. 1991. Tunnelling induced ground movements; predicting their magnitude and effects. In *Proceedings of the 4th International Conference on Ground Movements and Structures*, invited review paper, Cardiff, Pentech Press, London, : 671–697.

Rajesh, S. & Viswanadham, B. 2011. Hydro-mechanical behavior of geogrid reinforced soil barriers of landfill cover systems. *Geotextiles and Geomembranes* 29(1): 51–64.

Rajesh,S. & Viswanadham, B. 2012. Centrifuge Modeling and Instrumentation of Geogrid-Reinforced Soil Barriers of Landfill Covers. *Journal of Geotechnical and Geoenvironmental Engineering* 138(1): 26–37

Richards, D.J. and Powrie, W. 2011. Physical modelling of in-ground waste repository capping systems. *In Proceedings of the Institution of Civil Engineers-Waste and Resource Managemen*t (Vol. 164, No. 1, pp. 53-65).

Ross,S. 2013. *Simulation (5th Edition) - 10.3Latin Hypercube Sampling (5th ed.).* Elsevier Ltd

Rajesh, S. & Viswanadham, B. 2015. Numerical Simulation of Geogrid-Reinforced Soil Barriers Subjected to Differential Settlements. *International Journal of Geomechanics*, 15(4): 1–15

Singh, V.P., Jain, S.K. and Tyagi, A., 2007. *Risk and reliability analysis: a handbook for civil and environmental engineers*. ASCE, pp 131 – 132.

Tang, C.-S, Pei, X.-J, Wang, D.-Y, Shi, B., Li, J. 2014. Tensile Strength of Compacted Clayey Soil. *Journal of Geotechnical and Geoenvironmental Engineering* 141(4)

Thusyanthan, N., Take, W., Madabhushi, S., & Bolton, M. 2007. Crack initiation in clay observed in beam bending. *Geotechnique* 57(7): 581–594.

Viswanadham, B.V.S., and Rajesh, S. 2009. Centrifuge model tests on clay based engineered barriers subjected to differential settlements. *Applied Clay Science*. V42, p460 -472

Zeccos, D.P. 2005. *Evaluation of static and dynamic properties of municipal solid-waste*. PhD dissertation, University of California, Berkeley.